ACS Partner Journal

ENVIRONMENT & HEALTH

Open Access

pubs.acs.org/EnvHealth

Article

PFOS and Its Substitute OBS Cause Endothelial Dysfunction to Promote Atherogenesis in ApoE$^{-/-}$ Mice

Boxiang Zhang, Qing Li, Wensheng Wang, Mingming Tian, Dan Xu,* and Ying Xie*

Cite This: *Environ. Health* 2025, 3, 526−538

Read Online

ACCESS | Metrics & More | Article Recommendations | Supporting Information

ABSTRACT: Perfluorooctanesulfonate (PFOS), an emerging contaminant with widespread concern, has been associated with the pathogenesis of atherosclerosis (AS). As a substitute for PFOS, sodium p-perfluorous nonenoxybenzenesulfonate (OBS) is extensively utilized in various applications and detected in human blood. However, its potential health risk in AS remain unclear. In this study, we investigated the comparative impacts of PFOS and OBS on endothelial dysfunction and atherogenesis. In the *in vivo* study, Apolipoprotein E knockout (ApoE$^{-/-}$) mice were exposed to 0.4 or 4 mg/L PFOS/OBS for 12 weeks. We found that dyslipidemia developed more rapidly in the OBS-exposed mice than in the PFOS-exposed mice. PFOS exhibited a higher enrichment capacity in both blood and aortic tissues than OBS. Remarkably, OBS induced a more pronounced inflammatory response and caused a more significant disruption of the endothelial barrier in the aorta of ApoE$^{-/-}$ mice compared to PFOS. *In vitro* experiments showed that OBS, at the same exposure concentrations and durations as PFOS (0.1−20 μmol/L, 48 h), more effectively inhibited cell viability of human umbilical vein endothelial cells (HUVECs), caused higher levels of lactate dehydrogenase (LDH) release, and enhanced cell adhesion between HUVECs and monocytes. Both PFOS and OBS were found to activate the NF-κB signaling pathway and upregulate the expression of inflammatory factors. Notably, the use of OBS, but not PFOS, was shown to disrupt cell junctions and increase endothelial permeability by activating the MAPK/ERK signaling pathway. Our findings suggest that OBS may lead to endothelial dysfunction and have a greater impact on AS compared to PFOS, presenting significant health risks in cardiovascular diseases.

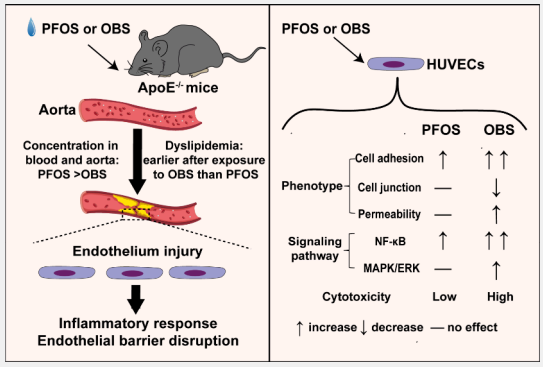

KEYWORDS: *PFOS, OBS, endothelial dysfunction, atherosclerosis, health risks*

1. INTRODUCTION

Pentafluorooctanesulfonate (PFOS) is one of perfluoroalkyl and polyfluoroalkyl substances (PFASs) with widespread concern. PFOS is characterized with environmental persistence, long-range transport, bioaccumulation and biomagnification, as well as broad range of toxic effects, leading to its global restriction or ban.[1] PFOS ranks the first in the list of emerging contaminants management in China at the beginning of 2023.[2] PFOS has been detected in various water bodies at concentrations ranging from 0.01 ng/L to 5 mg/L and is frequently found in soil, indoor and outdoor air, food, plants, and wildlife.[3] It was reported that PFOS was detected up to 85.90 ng/mL (0.17 μmol/L) in the blood of the adolescents and young (12 to 30 years old) and reached 10,400 ng/mL (20 μmol/L) in the blood of people living in Tangxun Lake of China.[4,5] PFOS has a variety of toxic effects on human health, including cardiovascular, neurotoxic, reproductive, hepatotoxic and immunotoxic impacts,[6−8] thereby closely associated with human diseases.[9]

Sodium p-perfluorous nonenoxybenzenesulfonate (OBS) acts as a substitute for PFOS, which is extensively applied in fire-fighting, oil extraction, and other industrial fields. The annual output of OBS in China is about 3,500 tons, and OBS has been frequently detected in the environment, including groundwater (7.25−59.89 ng/L), tap water (5.93−17.1 ng/L), and atmospheric particulate matter, especially with concentrations reaching 3.2 × 10^3 ng/L in river water around the Daqing Oil field.[10−15] Notably, OBS was detected in wild carp blood at the concentration of 144 ng/mL (0.23 μmol/L).[16] There is limited research on the presence of OBS in human blood, with only one study indicating that the concentration of OBS in the blood of pregnant women was found to be 0.711 ng/mL (0.001 μmol/L).[17] Recent reports show that OBS has a variety of toxicities, including neural toxicity, reproductive toxicity, developmental toxicity, intestinal toxicity, and liver toxicity.[18−21] OBS can bioaccumulate into the human body through various pathways; thereby, it is imperative to underscore the health risk of OBS.

Received: October 5, 2024
Revised: January 24, 2025
Accepted: January 30, 2025
Published: February 11, 2025

https://doi.org/10.1021/envhealth.4c00206
Environ. Health 2025, 3, 526−538

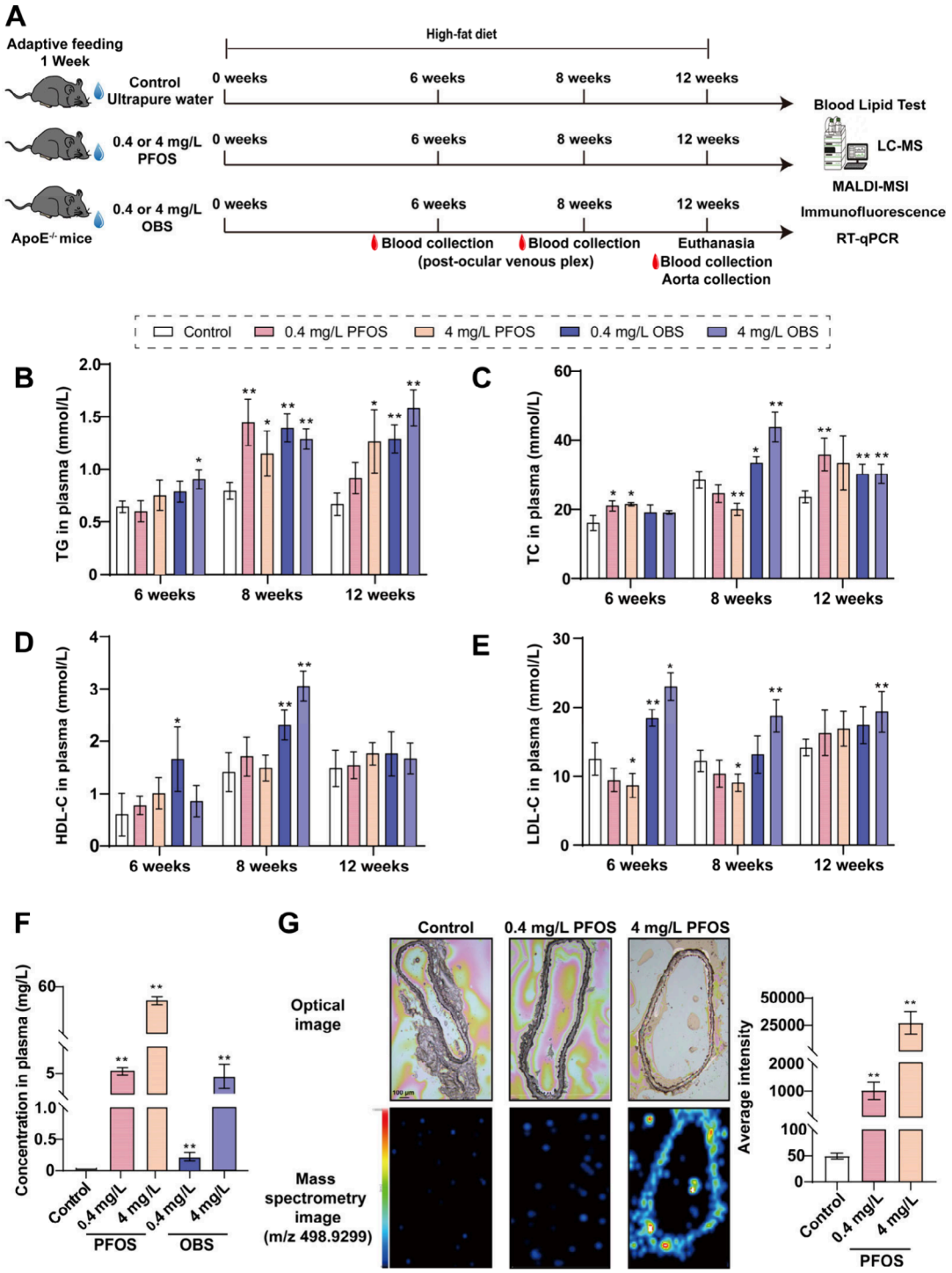

Figure 1. Effects of PFOS and OBS on the levels of blood lipids in ApoE$^{-/-}$ mice. (A) Flowchart of animal experimental procedure. (B–E) Levels of TG, TC, HDL-C, and LDL-C in plasma of mice at 6, 8, and 12 weeks postexposure (n = 4). (F) Levels of PFOS and OBS in plasma of mice at 12 weeks postexposure (n = 6). (G) Mass spectrometry images show the spatial distribution of PFOS in the aorta of mice, and average fluorescence intensity was quantitatively analyzed (n = 3). *P < 0.05, **P < 0.01. Scale bar: 100 μm.

Atherosclerosis (AS) is recognized as the primary cause of morbidity and mortality in the majority of cardiovascular diseases, and it is a significant contributor to acute cardiovascular events such as myocardial infarction and stroke.[22] It is known that vascular endothelial dysfunction plays an important role in the development and progression of AS.[23,24] Vascular endothelial cells are susceptible to stimulation by certain substances in the blood, leading to cell damage or dysfunction. When endothelial cells are subjected to persistent stimulation, an inflammatory cascade is initiated, leading to the upregulation of inflammatory mediators and adhesion molecules, as well as the recruitment of monocytes.[25] Concurrently, the disruption of endothelial cell junctions allows for the transmigration of lipoproteins into the intima layer, fostering the development of atherosclerotic plaques.[25] Furthermore, a metabolic imbalance between low-density lipoprotein (LDL)

https://doi.org/10.1021/envhealth.4c00206
Environ. Health 2025, 3, 526−538

and high-density lipoprotein (HDL) in the bloodstream is linked to endothelial cell dysfunction, which is a significant etiological factor in the development of AS.[26]

Emerging evidence suggests that PFOS exposure may affect the initiation and progression of AS.[27−29] Apolipoprotein E knockout ($ApoE^{-/-}$) mice serve as a prevalent model in AS research, which closely resembles human AS in terms of lesion distribution with their capacity to replicate hypercholesterolemia and the progression of AS.[30,31] *In vivo* investigations demonstrated that PFOS promoted arterial plaque formation, increased plaque vulnerability, and exacerbated AS lesions in $ApoE^{-/-}$ mice.[32] *In vitro* studies revealed that exposure to PFOS significantly increased cell permeability and compromised the integrity of tight junctions (TJs) in human microvascular endothelial cells.[33] In human umbilical vein endothelial cells (HUVECs), 200 μmol/L PFOS has been shown to incite inflammation and promote cell adhesion to monocytes.[34] Although there is a relative scarcity of research on the toxicity of OBS, exposure to 30 mg/L of OBS can adversely impact heart development and cause alterations in the vascular structure of zebrafish larvae. These effects manifest as a reduction in intersegmental vessel length and impaired dorsal longitudinal anastomotic vessel formation.[18] An assessment utilizing the Toxicological Priority Index (TPI) scores has suggested that OBS poses a higher health risk compared to PFOS.[35] However, the exact mechanisms and potential effects of PFOS and its novel substitute OBS on vascular endothelial function in AS remain to be elucidated.

In the present study, we performed both *in vivo* and *in vitro* experiments to investigate the impacts of PFOS and OBS on blood lipid levels, inflammatory responses and endothelial barrier function in the aortas of $ApoE^{-/-}$ mice. Concurrently, we assessed the distinct effects of PFOS and the OBS on endothelial dysfunction in HUVECs, focusing on cell viability, adhesion, permeability, and junctional integrity. Our findings suggest that both PFOS and OBS may pose substantial health risks in AS, indicating the necessity for further research into the safety profile of OBS as an alternative to PFOS in cardiovascular diseases.

2. MATERIALS AND METHODS

2.1. Animal Grouping and Experiment Design

Thirty adult male $ApoE^{-/-}$ mice (6 weeks old; Liaoning Changsheng biotechnology company, Benxi, China) were raised under specific pathogen free (SPF) conditions in a ventilated animal facility. $ApoE^{-/-}$ mice ($n = 6$) were randomly divided into five groups: Control, 0.4 mg/L PFOS, 4 mg/L PFOS, 0.4 mg/L OBS, and 4 mg/L OBS. Exposure concentrations of 0.4 and 4 mg/L were determined based on the maximum exposure concentration (4.6 mg/L) of PFOS in groundwater contaminated with PFASs.[36] We referenced previous PFOS exposure studies using a drinking water approach.[37] These exposure doses were approximated to 0.05−0.09 or 0.5−0.9 mg/kg/day, calculated for an average mouse weight of 30 g and an average daily water consumption of 4−7 mL. This work has received approval for research ethics from the Dalian Maritime University (No. DMU202401).

PFOS (CAS: 1763−23−1) and OBS (CAS: 70829−87−7) were purchased from Tokyo Chemical Industry Co., Ltd. (Tokyo, Japan) and Shanghai Futian Chemical Technology Co. (Shanghai, China), respectively. The flowchart of the animal experiment is shown in Figure 1A. After acclimatization for 1 week, all mice were reared on a high-fat diet including 20% fat by mass and 1.25% cholesterol (Jiangsu Xietong Pharmaceutical Bioengineering Company, Nanjing, China) for 12 weeks. During a 12 weeks exposure period, mice in the control group were given ultrapure water to drink. In contrast, those mice in the PFOS/OBS groups were administered a daily solution containing either 0.4 mg/L or 4 mg/L of PFOS/OBS dissolved in ultrapure water. Mouse body weights were monitored weekly, and food intake was recorded from weeks 6 to 12. Plasma samples were collected at weeks 6, 8, and 12 and stored at −80 °C for later analysis. Aortic samples were also collected at the end of the 12 weeks period and preserved at −80 °C until required for use. Plasma levels of total cholesterol (TC), triglycerides (TG), LDL-cholesterol (LDL-C), and HDL-cholesterol (HDL-C) were measured at weeks 6, 8, and 12 using specific assay kits (A111−1−1, A110−1−1, A113−1−1, A112−1−1, Nanjing Jianjian Bioengineering Institute, Nanjing, China).

2.2. Measurement of PFOS and OBS in Mice

PFOS and OBS concentrations in plasma were quantified using liquid chromatography-tandem mass spectrometry (LC-MS/MS) (Supporting Information for details). The distribution of PFOS in the aorta was visualized using matrix-assisted laser desorption/ionization mass spectrometry (MALDI-MSI, Shimadzu, Kyoto, Japan). Relative quantification was achieved by comparing the signal intensities across different regions, with the specific methodologies and calculation formulas detailed in the Supporting Information.

2.3. Immunofluorescent Staining

Vascular endothelial (VE)-cadherin in the aorta was monitored by immunofluorescent staining. Aortic tissues were first fixed in 4% paraformaldehyde for 24 h, followed by ethanol gradient dehydration and xylene hyalinization and finally paraffin embedding. Paraffin-embedded aortic tissues were cut into 5 μm thick sections with a microtome. Aortic paraffin sections were dewaxed to water and then antigenically repaired by using EDTA antigen repair buffer. Aortic tissue antigens were repaired and closed by serum for 30 min, and VE-cadherin antibody (ab205336, Abcam, Cambridge, UK) at a dilution of 1:1000 was added dropwise to the sections and incubated at 4 °C overnight. After the primary antibody incubation, the secondary antibody at a dilution of 1:200 (GB22301, Servicebio, Wuhan, China) was incubated at room temperature for 50 min. DAPI staining solution was added dropwise, incubated at room temperature for 10 min, and protected from light, and the film was sealed. Sections were placed under a scanner to capture images and analyzed for the percentage of positive area using image-J v1.53 software (National Institutes of Health, Bethesda, MA, USA)

2.4. Cell Culture and Exposure Experiments

HUVECs and human monocytic-leukemia cells (THP-1) were all purchased from the American type culture collection (ATCC). They were cultured in RPMI-1640 medium (C11875500BT, Gibco, GrandIsland, USA) supplemented with 10% FBS (FSP500, ExCell Bio, Suzhou, China). Cells were cultured at 37 °C and 5% CO_2 in an incubator. PFOS and OBS were dissolved in dimethyl sulfoxide (DMSO). Cells were treated with DMSO (0.1%), PFOS (0.01 to 200 μmol/L) or a diluted w/v OBS (0.01 to 100 μmol/L) for 24 or 48 h.

2.5. Cell Viability and LDH Release Assays

Cell viability and lactate dehydrogenase (LDH) release were measured using the 3-(4,5)-dimethylthiahiazo(-z-y1)-3,5-di-phenytetrazoliumromide (MTT) kit (KGA9301, KeyGEN BioTECH, Nanjing, China) and LDH Release Assay Kit (C0016, Beyotime, Shanghai, China), respectively. Briefly, HUVECs were seeded in 96-well plates (5000 cells per well), followed by exposure to different concentrations of PFOS or OBS for 24 or 48 h, and then the absorbance value was measured at 490 nm using a microplate reader (SpectraMa, Silicon Valley, USA).

2.6. Cell Adhesion Assay between HUVECs and THP-1 Cells

HUVECs were seeded in 6-well plates (9×10^4 cells per well) and exposed to PFOS or OBS for 48 h. THP-1 cells were labeled with BCECF-AM (S1006, Beyotime, China) and incubated for 30 min, and then 5×10^5 THP-1 cells per well were added into 6-well plates to coculture for 1 h with HUVECs. Nonadhered cells were rinsed using phosphate buffer saline (PBS) and the number of adherent cells were observed and recorded at an excitation wavelength of 488 nm/535 nm on a fluorescence microscope (Nikon, Tokyo, Japan). The number of

https://doi.org/10.1021/envhealth.4c00206
Environ. Health 2025, 3, 526−538

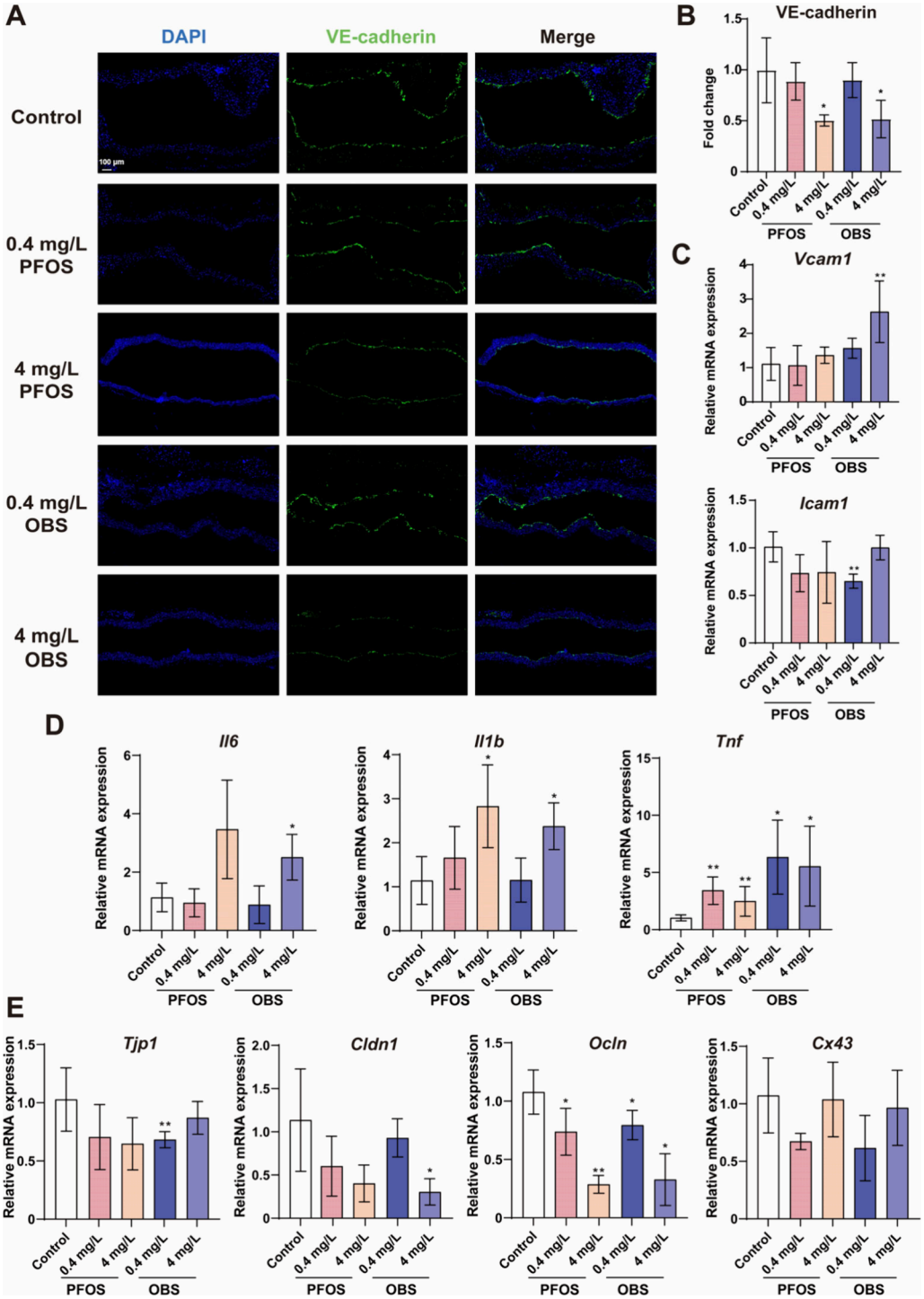

Figure 2. Effects of PFOS and OBS on vascular endothelium in the aorta of ApoE$^{-/-}$ mice. (A,B) Fluorescent images (A) and quantitative analysis (B) of VE-cadherin protein expression in aortic tissues of mice at 12 weeks after PFOS or OBS exposure. (C–E) Relative expression levels of cell adhesion molecules (C), inflammatory factors (D) and cell junction genes (E) determined using RT-qPCR in aortic tissues of mice at 12 weeks after PFOS or OBS exposure (n = 4). *P < 0.05, **P < 0.01. Scale bar: 100 μm.

adherent THP-1 cells (indicated by green dots) were counted in at least three randomly selected areas.

2.7. Cell Permeability and Gap Junction Assay

Cell permeability was evaluated by measuring apical-basolateral movements of FITC-dextran (40 kDa) (FD4, Sigma-Aldrich, St. Louis, MO, USA). Briefly, HUVECs were seeded in the insets of 24-well plates (1×10^5 cells per well), and reached 100% confluence. After cells were treated for 48 h, 2 mg/L FITC-dextran was added to inserts and cells were incubated for 2 h in the dark at 37 °C. Culture medium was collected from the upper and lower chambers at the end of the reaction, respectively. The fluorescence values were measured and recorded using a microplate reader at an excitation wavelength of 490 nm/520 nm. The permeability index was decided by comparing the FITC-dextran of the tracer between the upper chamber and the lower chamber.

Gap junction was evaluated by scrape loading assay using 0.05% lucifer yellow (L0144, Sigma-Aldrich). After cells were treated for 48 h, scratches were inflicted with a sterile scalpel and rinsed with PBS. Cells

https://doi.org/10.1021/envhealth.4c00206
Environ. Health 2025, 3, 526–538

were coincubated with lucifer yellow at 37 °C in the dark for 10 min. The fluorescence images were observed and photographed using a fluorescence microscope at an excitation wavelength of 470 nm/505 nm. The activity of the gap junction was quantified by measuring the maximum distance from the scratch line to the lucifer yellow leading edge.

2.8. Statistical Analysis

Data were presented as mean ± standard deviation (SD) derived from a minimum of three independent experiments. Statistical analyses were performed using GraphPad Prism 8.0.1 software (San Diego, CA, USA). For data adhering to a normal distribution, Student's *t* tests were employed for pairwise group comparisons, while one-way analysis of variance (ANOVA) was utilized for assessments involving multiple groups. In cases where the data did not follow a normal distribution, Kruskal–Wallis nonparametric tests were applied to assess differences between the PFOS/OBS-exposed groups and control. Statistical significance was set at $^{*}P < 0.05$ and $^{**}P < 0.01$.

3. RESULTS

3.1. The Distinct Effects of PFOS and OBS on Atherogenesis in ApoE$^{-/-}$ Mice

Dyslipidemia, a pivotal factor in the development of AS, is characterized by high levels of TG, TC and LDL-C, along with low levels of HDL-C. Therefore, we examined not only the changes in body weight and food intake during the exposure period but also assessed the lipid profiles of TG, TC, LDL-C and HDL-C in ApoE$^{-/-}$ mice after different durations of exposure to PFOS and OBS. A discernible reduction in body weight was observed in mice exposed to PFOS and OBS for up to 9 weeks (Figure S1A and S1B). A noticeable reduction in food intake was recorded at the 11th and 12th weeks following exposure to PFOS and OBS. (Figure S1C). Strikingly, exposure to OBS, but not PFOS, led to a pronounced increase in TG and LDL-C levels after 6 weeks, as compared to the control group (Figure 1B and 1E). Furthermore, TC and LDL-C levels were markedly higher at 8 weeks after OBS exposure, showing an approximate 2-fold increase relative to those observed following PFOS exposure (Figure 1C and 1E). HDL-C levels were significantly elevated at both 6 and 8 weeks after OBS exposure, in contrast to the negligible changes observed after PFOS exposure when compared to the control group (Figure 1D). These results suggest that OBS causes dyslipidemia at an earlier stage compared to that of PFOS.

It is well-known that ApoA-I and ApoB are protein biomarkers of AS, which are the main apolipoproteins of HDL and LDL, respectively. We conducted molecular docking experiments and found that both PFOS and OBS bind to either ApoA-I or ApoB. OBS and PFOS are capable of forming hydrogen bonds and halogen bonds with ApoA-I, respectively (Figure S2A and S2B). The combined stability of OBS and ApoA-I exceeds that of PFOS and ApoA-I, with binding energies of −6.2 and −6.0 kcal/mol, respectively. Importantly, the distances of these hydrogen and halogen bonds are all less than 3.5 Å. Furthermore, both OBS and PFOS can form hydrogen bonds with ApoB (Figure S2C and S2D). The combined stability of OBS and ApoB surpasses that of PFOS and ApoB, showing that their binding energies are −6.2 and −5.8 kcal/mol, respectively. ApoA-I interacts with cholesterol transporter proteins, facilitating the efflux of cholesterol and thus preventing plaque formation. Collectively, these findings imply that the binding of OBS and PFOS to apolipoproteins could potentially influence cholesterol transport, thereby contributing to the development of AS.

Further, we analyzed the concentration and accumulation of OBS and PFOS in the blood and aorta of ApoE$^{-/-}$ mice at the 12 weeks postexposure. The plasma concentration of OBS was found to be 0.22 mg/L (approximately 0.3 μmol/L) in the 0.4 mg/L exposure group and 4.39 mg/L (approximately 7 μmol/L) in the 4 mg/L exposure group, respectively. Correspondingly, the plasma concentration of PFOS was 5.41 mg/L (approximately 10 μmol/L) in the 0.4 mg/L exposure group and 44.8 mg/L (approximately 90 μmol/L) in the 4 mg/L exposure group (Figure 1F). The plasma concentration of OBS was nearly equivalent to the initial exposure concentration, whereas the PFOS levels were approximately 10-fold higher than the exposure concentration, indicating a greater propensity for PFOS to accumulate in the bloodstream compared to OBS. In MALDI-MSI analysis, OBS was not detected in the aorta of the exposed mice (Figure S3). In contrast, a significant enrichment of PFOS was observed in the aortas of mice, with increased intensity in both the 0.4 mg/L group and the 4 mg/L group (Figure 1G). We infer that this disparity may stem from the higher blood concentration of PFOS relative to OBS, leading to its accumulation in the aortic tissue.

3.2. PFOS and OBS Exposure Causes Endothelium Injury in the Aorta of ApoE$^{-/-}$ Mice

Endothelium injury is a pivotal event in the pathogenesis of AS. To assess the integrity of the vascular endothelium in the aorta, we examined the biomarkers that are indicative of endothelium injury. Immunofluorescent staining results showed that exposure to 4 mg/L PFOS or OBS led to a significant reduction in the cellular distribution of VE-cadherin along the cell membranes at intercellular junctions (Figure 2A). We also observed that VE-cadherin expression levels were significantly down-regulated in the aorta following exposure to 4 mg/L of either OBS or PFOS (Figure 2B). Regarding the expression of vascular cell adhesion molecule-1 (VCAM-1) and intercellular adhesion molecule-1 (ICAM-1), we observed a significant upregulation of *Vcam1* in the 4 mg/L of OBS group, while *Icam1* was notably downregulated in the 0.4 mg/L of OBS group. Interestingly, PFOS did not exert any influence on the mRNA expression levels of *Vcam1* and *Icam1* (Figure 2C). We further performed Immunohistochemical analysis in aortic tissues of mice to assess alterations in the protein expression levels of VCAM-1 and ICAM-1, and obtained similar results with RT-qPCR results (Figure S4). In terms of inflammatory factors, mRNA levels of interleukin-6 (*Il6*) and interleukin-1β (*Il1b*) were significantly upregulated in response to 4 mg/L of OBS exposure. Conversely, there was a noticeable trend of an increase in *Il6* and a clear upregulation of *Il1b* in the 4 mg/L PFOS group. The mRNA expression of tumor necrosis factor-α (*Tnf*) was significantly upregulated in the aorta after either PFOS or OBS exposure (Figure 2D). As for proteins associated with cell junctions, 0.4 mg/L of OBS significantly reduced zonula occluden-1(*Tjp1*) mRNA expression, and 4 mg/L of OBS considerably decreased Claudin-1 (*Cldn1*) mRNA expression in the aorta. The mRNA expression of Occludin-1 (*Ocln*) was significantly downregulated in the aorta after either PFOS or OBS exposure, while connexin43 (*Cx43*) exhibited a decreasing trend after exposure to OBS (Figure 2E).

3.3. The Distinct Effects of PFOS and OBS on Endothelial Cytotoxicity in HUVECs

It is known that vascular endothelial dysfunction plays a critical role in the development and progression of AS. Therefore, we explored the impacts of PFOS and OBS on endothelial

https://doi.org/10.1021/envhealth.4c00206
Environ. Health 2025, 3, 526−538

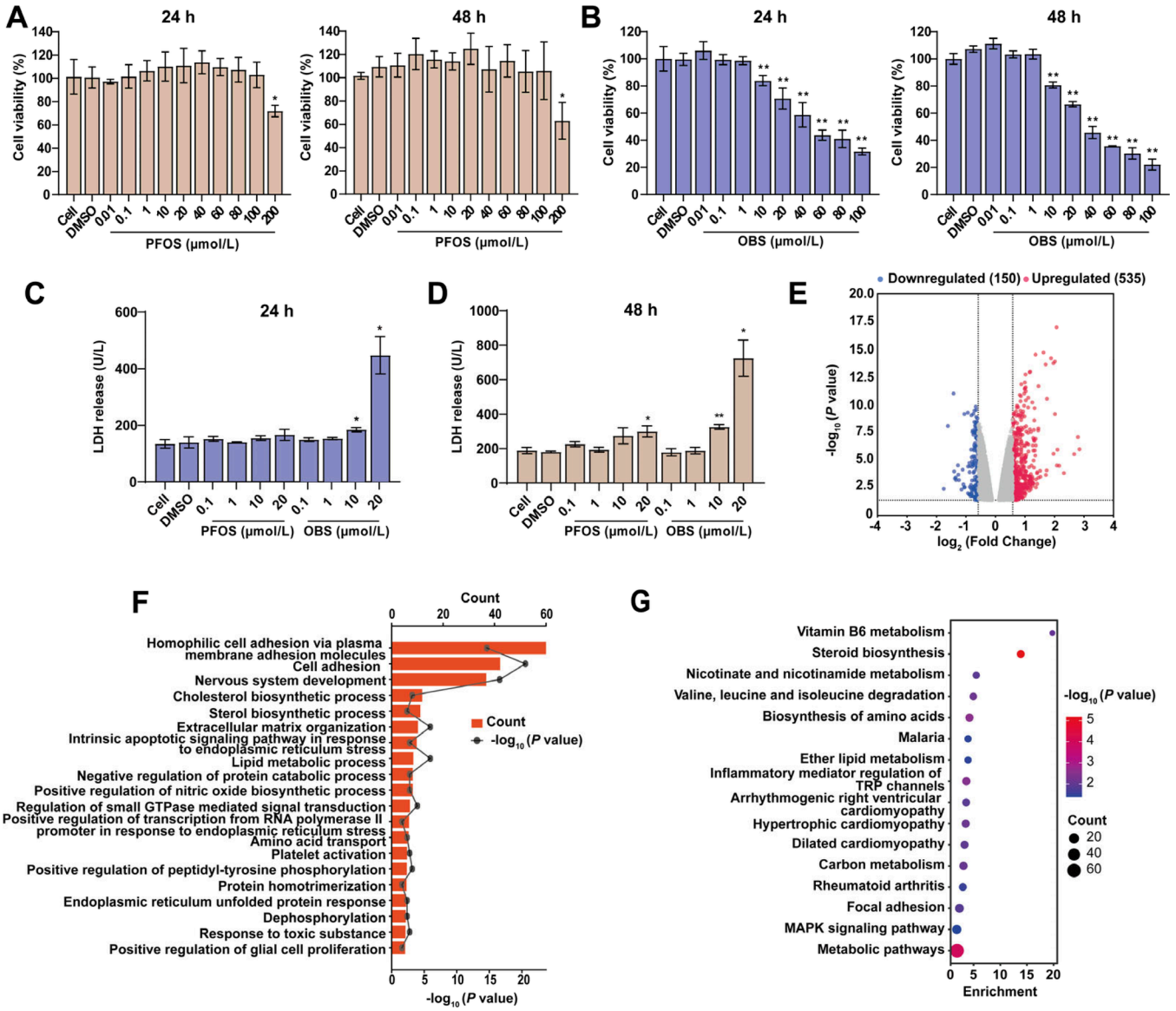

Figure 3. Effects of exposure to OBS on endothelial cytotoxicity and gene expression profile in HUVECs. (A-D) Cells were exposed to PFOS or an OBS for 24 and 48 h, followed by cell viability (A and B) and LDH release assays (C and D). (E) Volcano plots showed the changes in mRNA expression levels after cells were exposed to 20 μmol/L OBS for 48 h. (F) GO analysis of significantly upregulated genes was shown. (G) KEGG analysis of significantly upregulated genes was shown. $n = 3$, $^{*}P < 0.05$, $^{**}P < 0.01$.

cytotoxicity in HUVECs. The results showed that 200 μmol/L PFOS caused a significant reduction in cell viability (Figure 3A). In contrast, OBS significantly decreased cell viability in a dose-dependent manner, and 10 μmol/L of OBS exerted a pronounced inhibitory effect on cell viability (Figure 3B) at 24 and 48 h postexposure. Consequently, we selected a concentration range of 0.1 to 20 μmol/L for further experimental analysis. Consistent with the cell viability outcomes, PFOS (0.1−20 μmol/L) did not influence LDH release. However, the use of aqueous OBS (10 and 20 μmol/L) led to a significant increase in LDH release at 24 h after exposure (Figure 3C). The release of LDH was significantly increased after 48 h of exposure to 20 μmol/L of OBS or PFOS. Notably, the LDH release induced by OBS was approximately 3-fold that induced by PFOS (Figure 3D).

To further investigate the molecular mechanism underlying the cytotoxic effects of OBS in vascular endothelial cells, we analyzed mRNA expression profile in HUVECs. We examined the alterations in mRNA expression following a 48 h exposure to 20 μmol/L of OBS. In comparison to the control group, there were 685 differentially expressed genes, including 150 downregulated genes and 535 upregulated genes in the OBS-exposed group (Figure 3E). Gene Ontology (GO) analysis highlighted that the upregulated genes were significantly enriched in 46 biological processes, among which the top two processes are related to cell adhesion (Figure 3F). These upregulated genes are likely to exert their functions via the NF-κB signaling pathway (Table. S1). Conversely, the downregulated genes were significantly enriched in 23 biological processes, several of which are linked to GO terms related to mitochondrial function (Figure S5A). Further, KEGG enrichment analyses demonstrated that the upregulated genes were significantly enriched in 16 signaling pathways including the MAPK signaling pathway (Figure 3G). Meanwhile, the downregulated genes were significantly enriched in 14 signaling pathways including p53 signaling pathway and TNF-α signaling pathway (Figure S5B).

https://doi.org/10.1021/envhealth.4c00206
Environ. Health 2025, 3, 526−538

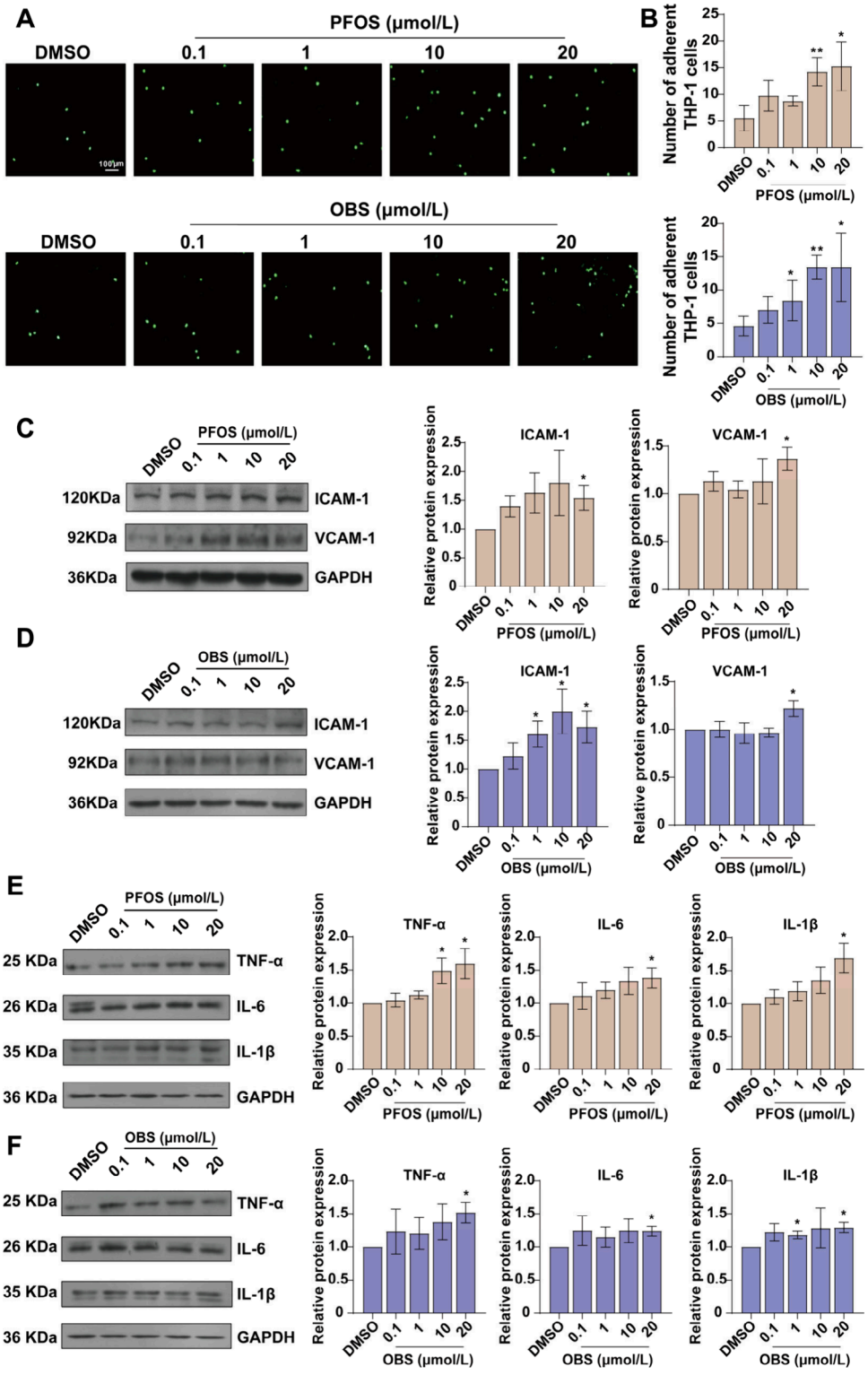

Figure 4. Impacts of PFOS and OBS on cell adhesion and inflammation in HUVECs. (A and B) Cell adhesion of THP-1 cells labeled with BCCF-AM to HUVECs were observed and the number of adhering cells were counted. (C−F) Representative Western blots were shown and protein expression levels of cell adhesion molecules and inflammation factors were quantified after exposure to PFOS (C and E) and OBS (D and F). $n = 3$, $^{*}P < 0.05$, $^{**}P < 0.01$. Scale bar: 100 μm.

These findings provide valuable insights into the molecular pathways that may be targeted by the OBS, potentially leading to endothelial dysfunction and cytotoxicity.

To explore the potential relationship between the exposure of a patient to OBS and human diseases, we first utilized the Comparative Toxicogenomic Database to identify 10 categories of human diseases associated with the exposure of a patient to OBS exposure. Based on the inference scores, we ranked these relevant diseases, including cardiovascular disease, cancer, diseases of nutrition and metabolism, respiratory disease and

https://doi.org/10.1021/envhealth.4c00206
Environ. Health 2025, 3, 526−538

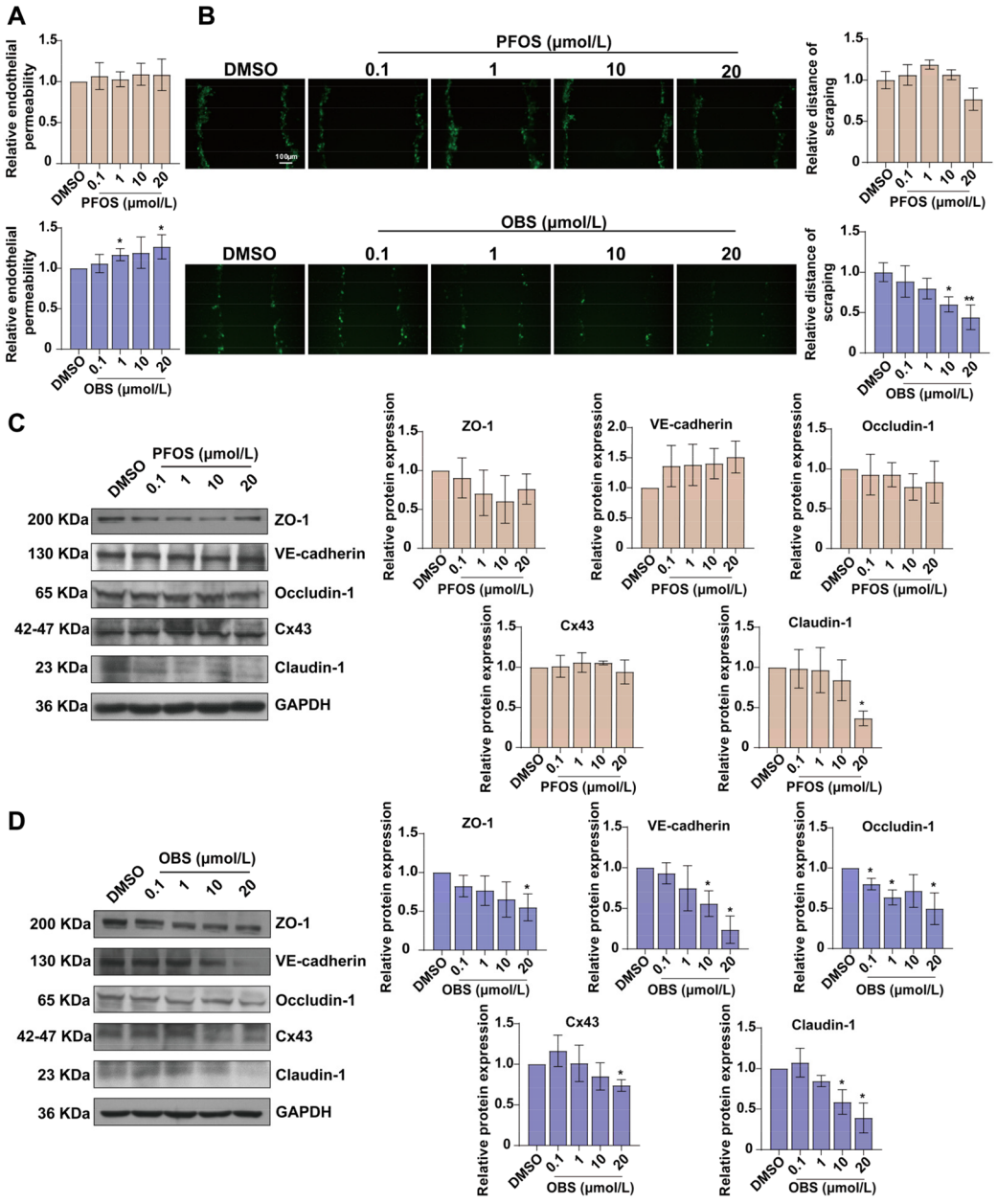

Figure 5. Effects of PFOS and OBS exposure on cell permeability and cell junctions in HUVECs. (A) Relative quantitative analysis of endothelial permeability after exposure to PFOS or OBS. (B) Representative fluorescence images of the gap junction assay, and relative distances of scrape after exposure to PFOS or OBS. (C and D) Representative Western blots, and relative expression levels of cell junction proteins after exposure to PFOS (C) or OBS (D). $n = 3$, $^{*}P < 0.05$, $^{**}P < 0.01$. Scale bar: 100 μm.

so on (Figure S6). Subsequently, to pinpoint the most probable cardiovascular diseases, we employed NextBio software for a more detailed prediction. Among the cardiovascular diseases, coronary arteriosclerosis emerged as the top disease with the highest score, indicating a strong association with OBS exposure (Table. S2).

3.4. The Distinct Effects of PFOS and OBS on Cell Adhesion and Inflammation in HUVECs

Cell adhesion between HUVECs and monocyte cells is one of the manifestations of endothelial cell injury and is thought as a major driver of AS. HUVECs were exposed to PFOS (0.1−20 μmol/L) or OBS (0.1−20 μmol/L) for 48 h, and followed by coculture with THP-1 monocyte cells. The results showed that both PFOS (10 μmol/L and 20 μmol/L) and OBS (1, 10, and 20 μmol/L) increased the number of THP-1 cells adhering to HUVECs (Figure 4A and 4B). Notably, the OBS significantly increased the number of adhesive cells in a dose-dependent manner. Western blot analysis revealed that the protein expression levels of ICAM-1 and VCAM-1 were significantly elevated when exposure to 20 μmol/L PFOS or OBS (Figure 4C and 4D). We found that OBS from 1 μmol/L to 20 μmol/L remarkably increased the protein expression levels of ICAM-1 (Figure 4D).

To investigate the impacts of PFOS and OBS on inflammatory factors and the NF-κB pathway in HUVECs, we performed Western blot analysis. The results demonstrated that exposure to 20 μmol/L of either PFOS or OBS led to a significant upregulation in the protein expression levels of TNF-α, IL-6 and IL-1β (Figure 4E and 4F). Specifically, 10 μmol/L

https://doi.org/10.1021/envhealth.4c00206
Environ. Health 2025, 3, 526−538

PFOS, but not OBS, was found to significantly enhance the protein expression level of TNF-α. Conversely, 1 μmol/L of OBS, but not PFOS, induced a significant increase in the protein expression level of IL-1β. Additionally, the expression levels of the phospho-IκBα (Ser32) were significantly upregulated by both PFOS (10 and 20 μmol/L) and OBS (20 μmol/L). However, no significant alterations were observed in the protein expression of total IκBα following exposure to either PFOS or OBS (Figure S7A and S7B).

3.5. The Distinct Effects of PFOS and OBS on Cell Permeability and Cell Junctions in HUVECs

Increase in endothelial cell permeability caused by the disruption of cell junctions is one of the important manifestations of endothelial dysfunction. HUVECs were exposed to PFOS (0.1−20 μmol/L) or OBS (0.1−20 μmol/L) for 48 h, followed by the determination of cell permeability and cell junctions. The results showed that PFOS had no effects on endothelial permeability and the gap junction. In contrast, OBS significantly increased endothelial permeability (Figure 5A), and diminished gap junction function in a dose-dependent manner (Figure 5B). Western blot analysis showed that protein expression levels of ZO-1, VE-cadherin, Occludin-1, Claudin-1 and Cx43 were significantly downregulated when exposed to OBS (Figure 5D), whereas 20 μmol/L PFOS only reduced the protein expression of Claudin-1 (Figure 5C).

It is reported that the activation of MAPK/ERK signaling pathway can increase cell permeability by downregulation of cell junction proteins such as ZO-1, occludins, and claudins.[38] In this study, KEGG enrichment analyses demonstrated that the upregulated genes were significantly enriched in the MAPK signaling pathway (Figure 3G). Therefore, we focused on MAPK signaling pathway to explore the potential mechanisms affecting cell permeability. We examined phospho-ERK and ERK protein expression levels after OBS and PFOS exposure in HUVECs. The results showed that OBS significantly led to the increase in the expression levels of phospho-ERK (Figure S8), indicating the activation of MAPK/ERK signaling pathway. We also observed the downregulation of cell junction proteins, including ZO-1, occluding-1, and claudin-1 in the OBS-exposed cells (Figure 5D). However, we did not detect the expression alterations in phospho-ERK and cell junction proteins in PFOS-exposed HUVECs.

4. DISCUSSION

PFOS is recognized as a hazardous chemical closely associated with cardiovascular diseases. With the prohibition of PFOS, its alternative, OBS, is increasingly being detected in the environment and human blood with great concern about health risks. In the present study, we examined the comparative effects of PFOS and its substitute, OBS, on endothelial dysfunction and atherogenesis by *in vivo* and *in vitro* experiments. We obtained key findings: OBS induced dyslipidemia earlier than PFOS did during atherogenesis. OBS had a lower enrichment capacity in blood and aorta compared to PFOS but caused more significant vascular endothelium injury at lower concentrations. OBS exhibited higher endothelial cytotoxicity and promoted monocyte-endothelial cell adhesion at concentrations lower than those of PFOS. OBS, not PFOS, disrupted cell junctions and increased permeability in HUVECs via the MAPK/ERK signaling pathway. These findings reveal that the presence of OBS is more likely to contribute to AS compared to PFOS, indicating the potential health risks of the presence of OBS in cardiovascular diseases.

Abnormal lipid metabolism is an important cause of AS plaque formation, and dyslipidemia is often recognized in the early stages of AS. Genetic deletion of ApoE in mice results in increased levels of plasma cholesterol, leading to hypercholesterolemia. ApoE$^{-/-}$ mice are extensively used in AS research due to their ability to model hypercholesterolemia, AS development, and the interplay between inflammation and lipoprotein metabolism, which are all critical aspects of cardiovascular disease research.[30] In this study, we established an AS model in ApoE$^{-/-}$ mice that shows a significant increase in TG, TC, and LDL-C levels and an obvious decrease in HDL levels compared to wild-type mice (data not shown). We found that both PFOS and OBS resulted in the remarkable increase in TG, TC, and LDL-C levels in ApoE$^{-/-}$ mice. We noted a marked elevation in LDL-C concentration in the OBS group compared to the PFOS group at week 6 under identical exposure conditions. At week 8, the levels of both LDL-C and TC were significantly higher in the OBS group than in the PFOS group (Figure S9A and S9B). OBS caused dyslipidemia earlier than PFOS during atherogenesis in ApoE$^{-/-}$ mice, indicating that OBS may have a more rapid and potent effect on lipid metabolism disruption and the initiation of AS processes compared to PFOS.

Apolipoprotein is one of the plasma lipoproteins that can bind and transport blood lipids to various tissues of the body for metabolism and utilization, which can affect the occurrence and development of AS.[39] ApoA-I is one of the main components of HDL, which is responsible for collection and transport of cholesterol from tissues and vessel walls back to the liver, participating in the reverse transport of cholesterol in the body.[40] We found here that both PFOS and OBS can bind to ApoA-I, and the binding stability of the OBS is slightly higher than that of the PFOS, which might contribute to the increase in TG levels in PFOS/OBS exposed mice and elevated HDL-C levels in OBS-exposed mice (Figure 1). ApoB is the main building blocks of LDL, which clears the remnants of lipid metabolism through endocytosis mediated by LDL receptor (LDLR) on the surface of liver cells.[41] Interestingly, the binding sites of PFOS and OBS with ApoB are located at the LDLR position and may impede the degradation of LDL to increase plasma LDL concentrations. Epidemiological investigations reports revealed a remarkable positive association between PFOS concentrations and LDL levels in the blood.[42] These findings indicate that PFOS and OBS may influence cholesterol transport and disrupt the normal degradation process of LDL, thereby raising the risk of cardiovascular diseases.

A number of studies demonstrate that PFOS and OBS have a variety of toxicities. In comparison of toxicity between PFOS and OBS, PFOS exhibits more potent toxic effects than OBS, including aquatic toxicity, development toxicity, neurotoxicity, liver toxicity.[43,18,44,21] PFOS can bind with PPARγ to induce liver metabolic disorders and disrupt the lipid metabolism balance. OBS cannot bind with PPARγ, but affect lipid gene and amino acid, so that interfere liver metabolic balance.[44] They have hepatotoxicity, but OBS has a greater cytotoxicity than PFOS in HepG2 cells. PFOS (300−400 μmol/L) slightly inhibits the cell viability and disrupts the cell membrane in HepG2 cells. OBS (from 80 μmol/L) obviously inhibits cell growth and induces lipid accumulation in HepG2 cells.[45] In the present study, OBS caused more significant vascular endothelium injury in mice and exhibited higher endothelial cytotoxicity

https://doi.org/10.1021/envhealth.4c00206
Environ. Health 2025, 3, 526−538

in HUVECs than in PFOS (Figures 1−3). At equivalent concentration, OBS caused a pronounced reduction in cell viability and a significant increase in LDH release in comparison to PFOS, indicating that the endothelial cytotoxicity of OBS in HUVECs was significantly higher than that of PFOS (Figure S9C and S9D). Particularly, the presence of OBS, not PFOS, disrupted cell junctions and increased endothelial permeability in the *in vivo* and *in vitro* experiments (Figure 5). Our findings suggest that PFOS and OBS have endothelial toxicity, but OBS has greater cytotoxicity than PFOS in HUVECs.

Both PFOS and OBS are capable of bioaccumulating within organisms through multiple pathways, but PFOS exhibits a more potent ability to accumulate compared to OBS. After 21 days of exposure to 1 μmol/L OBS or PFOS, the concentration of PFOS in zebrafish liver was approximately 5-fold higher than that of OBS, suggesting that PFOS might be more readily enriched compared to OBS.[19] The Bioconcentration Factor (BCF) for PFOS is notably higher, due to its powerful binding affinity to specific proteins compared to OBS.[46,47] In studies involving zebrafish larvae, the uptake rate constants for OBS were comparable to those of PFOS, but the elimination rate constants for OBS were significantly higher than those of PFOS.[46] In the present study, ApoE$^{-/-}$ mice were exposed to equivalent concentrations of PFOS and OBS, yet the enrichment of OBS in the blood and aorta of mice was substantially lower than that of PFOS after 12 weeks of exposure (Figure 1), which might be attributed to the difference in the elimination rates between PFOS and OBS within the body. In addition, we detected that the plasma concentration of OBS was 0.22 mg/L (approximately 0.3 μmol/L) in the 0.4 mg/L group and 4.39 mg/L (approximately 7 μmol/L) in the 4 mg/L group, respectively. The concentration of OBS in plasma was detected to be close to the initial exposure concentration of OBS. The concentration of 0.4 mg/L PFOS was 5.41 mg/L (approximately 10 μmol/L) in plasma at 12 weeks after exposure in mice. The concentration of PFOS in plasma was approximately 10 times as high as the exposure concentration, suggesting that PFOS might more readily enriched in the blood in comparison to OBS, which results in the accumulation of PFOS in the aorta and thus the spatial distribution of PFOS in the mouse aorta was detected easier than OBS.

Endothelial dysfunction is considered a key early step in the development of AS. It plays a crucial role in the initiation and progression of AS through various mechanisms that include promoting the expression of adhesion molecules, increasing chemokine secretion, augmenting leukocyte adhesion, and enhancing low-density lipoprotein oxidation.[25] VCAM-1 and ICAM-1 are important cell adhesion molecules, which contribute to mediating leukocyte migration and endothelial cell adhesion during inflammation.[48] The protein expression of VCAM-1 and inflammatory factors (IL-6, IL-1β and TNF-α) were upregulated when ApoE$^{-/-}$ mice or HUVECs were exposed to PFOS or OBS (Figures 2 and 4). No significant disparities were observed in the expression levels of cell adhesion molecules and inflammation factors between 20 μmol/L PFOS group and 20 μmol/L OBS group (Figure S9E). We found that ICAM-1 was upregulated in HUVECs exposed to PFOS or OBS, but not in animal experiments. The discrepancies observed between *in vitro* and *in vivo* studies could stem from the varying levels of PFOS and OBS present in HUVECs and within the aortic tissues of mice. It is reported that 200 μmol/L PFOS significantly promoted cell adhesion between THP-1 monocytes and HUVECs,[34] whereas our results showed that 10 μmol/L PFOS and 1 μmol/L OBS promoted cell adhesion between THP-1 monocytes and HUVECs (Figure 4A and 4B). The NF-κB signaling pathway serves as a central regulatory hub for inflammatory gene expression. Phosphorylated IκBα (p-IκBα) triggers the release and activation of NF-κB, which in turn, enhances the transcription of inflammatory mediators.[49] Our findings revealed that exposure to both PFOS and OBS led to an increase in the expression of p-IκBα, suggesting that activation of the NF-κB signaling pathway plays a role in positively modulating inflammatory responses and enhancing cell adhesion. Additionally, research drawing from the National Health and Nutrition Examination Survey (NHANES) identified IL-6, IL-1β and TNF-α as key genes in the inflammatory response triggered by PFASs.[50] Notably, PFOS demonstrated a significant positive correlation with inflammation-related proteins, potentially contributing to the development of coronary artery disease, particularly in postmenopausal women.[51]

An increase in endothelial permeability is one of important characteristics for endothelial injury, providing a necessary condition for LDL to pass through the endothelial barrier in AS progression.[26] Previous studies indicated that exposure to 12.5 μmol/L PFOS did not affect cell permeability in human brain microvascular endothelial cells (HBMECs), whereas 50 μmol/L PFOS led to a reduction in permeability and disrupted the blood-brain barrier.[52] Another study reported that cell permeability was significantly enhanced by 5 μmol/L PFOS in human microvascular endothelial cells.[33] In our study, we observed that OBS, at concentrations ranging from 1 to 20 μmol/L, significantly increased endothelial cell permeability, while PFOS does not impact cell permeability in HUVECs. These findings suggest that OBS has a distinct effect on vascular endothelial permeability compared to PFOS. OBS may have a more pronounced impact on vascular integrity and could potentially lead to vascular injury or dysfunction. The differential response to PFOS and OBS highlights the importance of considering the specific chemical properties and concentrations of PFASs when assessing their effects on endothelial cell function and vascular health.

Cell junctions serve as the primary mechanism to prevent "leakage" of the endothelial barrier, primarily achieved through adhesion junctions, gap junctions, and tight junctions.[53] VE-cadherin is a strictly endothelial-specific adhesive molecule located at the adhesion junctions. Reduction in VE-cadherin mediates the increase in cell permeability and the passage of leukocytes across the endothelial barrier.[54] In this study, we observed that 4 mg/L PFOS and OBS reduced expression levels of VE-cadherin in *vivo* experiments, implying that PFOS and OBS disrupted the integrity of vascular endothelium. However, VE-cadherin was significantly downregulated when exposure to 10 and 20 μmol/L OBS rather than PFOS in HUVECs (Figures 5 and S9F). Among the 21 types of gap junction proteins, Cx43 is the widest distribution protein in the human body, which is essential in the regulation of endothelial cell permeability.[55] We observed a decreasing trend of Cx43 in mouse aorta and downregulation of Cx43 in HUVECs after OBS exposure (Figures 2 and 5). OBS diminished gap junction function in HUVECs (Figure 5). However, we confirmed that PFOS did not affect Cx43 expression in *in vivo* and *in vitro* experiments. The tight junctions are mainly comprised of transmembrane proteins such as Occludin and Claudin, and cytoplasmic proteins such as occludins, namely ZO-1−3. Occludin is able to close the paracellular pathway, involved in maintaining and regulating the

https://doi.org/10.1021/envhealth.4c00206
Environ. Health 2025, 3, 526−538

barrier function.[56] Claudin can form paracellular "pores," which can selectively regulate the passage of substances, especially ions.[57] ZO-1 can link transmembrane proteins to form complexes, maintaining the barrier function.[38] Previous studies found that protein expression of occludin-1 and claudin-5 were significantly downregulated by exposure to 20 μmol/L PFOS in HBMECs.[52] Our results demonstrated that OBS significantly downregulated ZO-1, Occulin-1 and Claudin-1 in ApoE$^{-/-}$ mice and HUVECs. In contrast, PFOS decreased only Claudin-1 protein expression in HUVECs and downregulated the expression of Occulin-1 in ApoE$^{-/-}$ mice (Figures 2 and 5), which may be due to the difference in exposure concentrations and exposure time.

It is reported that the activation of MAPK/ERK signaling pathway can increase cell permeability by downregulation of cell junction proteins such as ZO-1, occludins, and claudins.[38] MAPK signaling is achieved through phosphorylation cascade, in which ERK is one of the important kinases in the process.[58] It has been found that lipopolysaccharide can activate ERK to downregulate claudin-5, occludin, and ZO-1, thereby increasing human lung microvascular permeability.[59] Furthermore, H_2O_2-induced activation of Phospholipase C resulted in activation of ERK1/2 and increased paracellular permeability by downregulation of occludin, ZO-1, and ZO-2.[60] 15(S)-Hydroxyeicosatetraenoic Acid Partly can cause ZO-1 phosphorylation via PKC activation of MEK1-ERK1/2, leading to dissociation of ZO-1 from occludin and disruption of vascular endothelial barrier function.[61] In this study, KEGG enrichment analyses demonstrated that the upregulated genes were significantly enriched in MAPK signaling pathway (Figure 3G). OBS significantly led to the increase in the expression levels of phospho-ERK, indicating the activation of MAPK/ERK signaling pathway. We also observed the downregulation of cell junction proteins, including ZO-1, occluding-1, and claudin-1 in OBS-exposed cells. However, PFOS did not activate the MAPK/ERK signaling pathway in the HUVECs. These findings indicate that the vascular injury induced by OBS influences the integrity of adhesion junctions, gap junctions, and tight junctions by activating the MAPK/ERK signaling pathway, which results in increased permeability of HUVECs and, consequently, vascular injury. In contrast, PFOS at equivalent concentrations did not induce vascular injury, suggesting a differential impact on vascular endothelial function.

5. CONCLUSION

In this study, we found that both PFOS and its substitute, OBS, induce endothelial dysfunction to promote atherogenesis. PFOS exhibited a greater propensity for enrichment in the bloodstream and accumulation in the aorta of mice in comparison to OBS. Notably, OBS induced dyslipidemia at an early stage of AS and caused more significant endothelial injury in ApoE$^{-/-}$ mice than PFOS. OBS was significantly higher than that of PFOS in HUVECs. Importantly, the OBS, rather than PFOS, disrupted cell junctions, leading to increased endothelial permeability through the activation of the MAPK/ERK signaling pathway. These findings suggest that OBS has greater health risks than PFOS in AS, providing valuable insights for further assessment of its safety as a PFOS substitute, particularly in relation to cardiovascular diseases.

■ ASSOCIATED CONTENT

Data Availability Statement

Data will be made available on request.

Supporting Information

The Supporting Information is available free of charge at https://pubs.acs.org/doi/10.1021/envhealth.4c00206.

Materials and methods including association analysis between OBS and human diseases, PFOS and OBS concentration measurements in plasma, MALDI−MSI analysis, RNA isolation and RT-qPCR analyse,: RNA-seq analysis, Western blot analysis, molecular docking analysis; results including effects of PFOS or OBS exposure on body weight and food intake in ApoE$^{-/-}$ mice, PFOS and OBS bind to ApoA-I or ApoB in molecular docking experiments, representative images of aorta after exposure to OBS in MALDI−MS analysis, effects of PFOS and OBS on VCAM-1 and ICAM-1 expression in the aorta of ApoE$^{-/-}$ mice, GO analysis and KEGG analysis of differentially expressed genes, predictive analysis of association between OBS and human diseases, effects of PFOS or OBS on NF-κB pathway in HUVECs, effects of PFOS or OBS on MAPK/ERK pathway in HUVECs, comparative analysis of the effects of PFOS and OBS in ApoE$^{-/-}$ mice and HUVECs, ion flow and standard curve of PFOS and OBS in LC-MS and MALDI−MSI analysis, GO enrichment analysis of differentially expressed genes when exposure to OBS, top 5 diseases in CVD predicted to be associated with OBS, experimental conditions for chromatographic analysis and mass spectrometry, information of primers for quantitative RT-qPCR and information on antibodies used in Western blot analysis (PDF)

■ AUTHOR INFORMATION

Corresponding Authors

Dan Xu − *Institute of Environmental Systems Biology, Environment Science and Engineering College, Dalian Maritime University, Dalian 116026, China*; orcid.org/0000-0002-4645-2665; Email: jotan1995@163.com

Ying Xie − *The Second Affiliated Hospital of Dalian Medical University, Dalian 116023, China*; Email: 936135710@qq.com

Authors

Boxiang Zhang − *Institute of Environmental Systems Biology, Environment Science and Engineering College, Dalian Maritime University, Dalian 116026, China*

Qing Li − *Institute of Environmental Systems Biology, Environment Science and Engineering College, Dalian Maritime University, Dalian 116026, China*

Wensheng Wang − *Institute of Environmental Systems Biology, Environment Science and Engineering College, Dalian Maritime University, Dalian 116026, China*

Mingming Tian − *Institute of Environmental Systems Biology, Environment Science and Engineering College, Dalian Maritime University, Dalian 116026, China*

Complete contact information is available at: https://pubs.acs.org/10.1021/envhealth.4c00206

Author Contributions

Boxiang Zhang: Methodology, Investigation, Writing-original draft; **Qing Li:** Investigation, Data curation; **Wensheng Wang:** Investigation, Methodology; **Mingming Tian:** Writing-review editing, Supervision; **Dan Xu:** Conceptualization, Writing-review editing, Supervision, Project administration. **Ying Xie:** Investigation, Supervision.

Notes

The authors declare no competing financial interest.

■ ACKNOWLEDGMENTS

This work was supported by National Natural Science Foundation of China (No. 42077382) and the Fundamental Research Funds for the Central Universities (3132023528, 3132023160). We thank the support for RNA sequencing analysis from Wuhan SeqHealth Tech Co., Ltd. in Hubei, China. We thank the Shimadzu Beijing Analysis Center for its support of the MALDI-MSI analysis.

■ REFERENCES

(1) Podder, A.; Sadmani, A.; Reinhart, D.; Chang, N. B.; Goel, R. Per and poly-fluoroalkyl substances (PFAS) as a contaminant of emerging concern in surface water: A transboundary review of their occurrences and toxicity effects. *J. Hazard. Mater.* **2021**, *419*, 126361.

(2) Wang, Y.; Jiang, L.; Jiang, G. Emerging Chemicals in China: Historical Development, Current Situation, and Future Outlook. *Environment & Health.* **2024**, *2* (4), 180−188.

(3) Johnson, G. R.; Brusseau, M. L.; Carroll, K. C.; Tick, G. R.; Duncan, C. M. Global distributions, source-type dependencies, and concentration ranges of per - and polyfluoroalkyl substances in groundwater. *Sci. Total Environ.* **2022**, *841*, 156602.

(4) Lin, C.; Lin, L.; Wen, T.; Lien, G.; Chien, K.; Hsu, S. H. J.; Liao, C.; Sung, F.; Chen, P.; Su, T. Association between levels of serum perfluorooctane sulfate and carotid artery intima-media thickness in adolescents and young adults. *Int. J. Cardiol.* **2013**, *168* (4), 3309−3316.

(5) Zhou, Z.; Shi, Y.; Vestergren, R.; Wang, T.; Liang, Y.; Cai, Y. Highly elevated serum concentrations of perfluoroalkyl substances in fishery employees from Tangxun lake, china. *Environ. Sci. Technol.* **2014**, *48* (7), 3864−3874.

(6) Antonopoulou, M.; Spyrou, A.; Tzamaria, A.; Efthimiou, I.; Triantafyllidis, V. Current state of knowledge of environmental occurrence, toxic effects, and advanced treatment of PFOS and PFOA. *Sci. Total Environ.* **2024**, *913*, 169332.

(7) Xuan, R.; Qiu, X.; Wang, J.; Liu, S.; Magnuson, J. T.; Xu, B.; Qiu, W.; Zheng, C. Hepatotoxic response of perfluorooctane sulfonamide (PFOSA) in early life stage zebrafish (Danio rerio) is greater than perfluorooctane sulfonate (PFOS). *J. Hazard. Mater.* **2024**, *461*, 132552.

(8) Li, H.; Yang, M.; Zhao, J.; Tan, Z.; Li, L.; An, Z.; Liu, Y.; Liu, X.; Zhang, X.; Lu, J.; Li, A.; Guo, H. Association of Per- and Polyfluoroalkyl Substance Exposure with Coronary Stenosis and Prognosis in Acute Coronary Syndrome. *Environment & Health.* **2024**, DOI: 10.1021/envhealth.4c00166.

(9) Shi, W.; Zhang, Z.; Li, M.; Dong, H.; Li, J. Reproductive toxicity of PFOA, PFOS and their substitutes: A review based on epidemiological and toxicological evidence. *Environ. Res.* **2024**, *250*, 118485.

(10) Bao, Y.; Qu, Y.; Huang, J.; Cagnetta, G.; Yu, G.; Weber, R. First assessment on degradability of sodium p - perfluorous nonenoxybenzene sulfonate (OBS), a high volume alternative to perfluorooctane sulfonate in fire-fighting foams and oil production agents in China. *Rsc Adv.* **2017**, *7* (74), 46948−46957.

(11) Xu, L.; Shi, Y.; Li, C.; Song, X.; Qin, Z.; Cao, D.; Cai, Y. Discovery of a Novel Polyfluoroalkyl Benzenesulfonic Acid around Oilfields in Northern China. *Environ. Sci. Technol.* **2017**, *51* (24), 14173−14181.

(12) Yu, N.; Guo, H.; Yang, J.; Jin, L.; Wang, X.; Shi, W.; Zhang, X.; Yu, H.; Wei, S. Non-Target and Suspect Screening of Per- and Polyfluoroalkyl Substances in Airborne Particulate Matter in China. *Environ. Sci. Technol.* **2018**, *52* (15), 8205−8214.

(13) Chen, H.; Munoz, G.; Duy, S. V.; Zhang, L.; Yao, Y.; Zhao, Z.; Yi, L.; Liu, M.; Sun, H.; Liu, J.; Sauve, S. Occurrence and Distribution of Per- and Polyfluoroalkyl Substances in Tianjin, China: The Contribution of Emerging and Unknown Analogues. *Environ. Sci. Technol.* **2020**, *54* (22), 14254−14264.

(14) Shi, Y.; Song, X.; Jin, Q.; Li, W.; He, S.; Cai, Y. Tissue distribution and bioaccumulation of a novel polyfluoroalkyl benzenesulfonate in crucian carp. *Environ. Int.* **2020**, *135*, 105418.

(15) Jiao, E.; Zhu, Z.; Yin, D.; Qiu, Y.; Karrman, A.; Yeung, L. A pilot study on extractable organofluorine and per- and polyfluoroalkyl substances (PFAS) in water from drinking water treatment plants around Taihu Lake, China: what is missed by target PFAS analysis? *Environ. Sci.-Process Impacts.* **2022**, *24* (7), 1060−1070.

(16) Hou, M.; Jin, Q.; Na, G.; Cai, Y.; Shi, Y. Emissions, Isomer-Specific Environmental Behavior, and Transformation of OBS from One Major Fluorochemical Manufacturing Facility in China. *Environ. Sci. Technol.* **2022**, *56* (12), 8103−8113.

(17) Li, Y.; Yu, N.; Du, L.; Shi, W.; Yu, H.; Song, M.; Wei, S. Transplacental Transfer of Per - and Polyfluoroalkyl Substances Identified in Paired Maternal and Cord Sera Using Suspect and Nontarget Screening. *Environ. Sci. Technol.* **2020**, *54* (6), 3407−3416.

(18) Huang, J.; Sun, L.; Mennigen, J. A.; Liu, Y.; Liu, S.; Zhang, M.; Wang, Q.; Tu, W. Developmental toxicity of the novel PFOS alternative OBS in developing zebrafish: An emphasis on cilia disruption. *J. Hazard. Mater.* **2021**, *409*, 124491.

(19) Wang, C.; Weng, Y.; Tu, W.; Jin, C.; Jin, Y. Maternal exposure to sodium rho-perfluorous nonenoxybenzene sulfonate during pregnancy and lactation disrupts intestinal barrier and may cause obstacles to the nutrient transport and metabolism in F0 and F1 generations of mice. *Sci. Total Environ.* **2021**, *794*, 148775.

(20) Wang, C.; Fang, C.; Wang, C.; Jin, C.; Qian, M.; Jin, Y. Maternal Sodium p-Perfluorous Nonenoxybenzene Sulfonate Exposure Disturbed Lipid Metabolism and Induced an Imbalance in Tyrosine Metabolism in the F1 Generation of Mice. *Chem. Res. Toxicol.* **2022**, *35* (4), 651−662.

(21) Wang, Q.; Gu, X.; Liu, Y.; Liu, S.; Lu, W.; Wu, Y.; Lu, H.; Huang, J.; Tu, W. Insights into the circadian rhythm alterations of the novel PFOS substitutes F-53B and OBS on adult zebrafish. *J. Hazard. Mater.* **2023**, *448*, 130959.

(22) Clifford, A. H.; Cohen Tervaert, J. W. Cardiovascular events and the role of accelerated atherosclerosis in systemic vasculitis. *Atherosclerosis.* **2021**, *325*, 8−15.

(23) Godo, S.; Shimokawa, H. Endothelial Functions. *Arterioscler. Thromb. Vasc. Biol.* **2017**, *37* (9), No. e108-e114.

(24) Augustin, H. G.; Koh, G. Y. A systems view of the vascular endothelium in health and disease. *Cell.* **2024**, *187* (18), 4833−4858.

(25) Bjorkegren, J.; Lusis, A. J. Atherosclerosis: Recent developments. *Cell.* **2022**, *185* (10), 1630−1645.

(26) Mundi, S.; Massaro, M.; Scoditti, E.; Carluccio, M. A.; van Hinsbergh, V.; Iruela-Arispe, M. L.; De Caterina, R. Endothelial permeability, LDL deposition, and cardiovascular risk factors-a review. *Cardiovasc. Res.* **2018**, *114* (1), 35−52.

(27) Lin, C. Y.; Lin, L. Y.; Wen, T. W.; Lien, G. W.; Chien, K. L.; Hsu, S. H.; Liao, C. C.; Sung, F. C.; Chen, P. C.; Su, T. C. Association between levels of serum perfluorooctane sulfate and carotid artery intima-media thickness in adolescents and young adults. *Int. J. Cardiol.* **2013**, *168* (4), 3309−3316.

(28) Lin, C.; Chen, P.; Lo, S.; Torng, P.; Sung, F.; Su, T. The association of carotid intima-media thickness with serum Level of perfluorinated chemicals and endothelium-platelet microparticles in adolescents and young adults. *Environ. Int.* **2016**, *94*, 292−299.

(29) Lin, C.; Lee, H.; Hwang, Y.; Su, T. The association between total serum isomers of per - and polyfluoroalkyl substances, lipid profiles, and the DNA oxidative/nitrative stress biomarkers in middle-aged Taiwanese adults. *Environ. Res.* **2020**, *182*, 109064.

(30) Oppi, S.; Luscher, T. F.; Stein, S. Mouse Models for Atherosclerosis Research-Which Is My Line? *Front. Cardiovasc. Med.* **2019**, *6*, 46.
(31) Jawien, J.; Nastalek, P.; Korbut, R. Mouse models of experimental atherosclerosis. *J. Physiol. Pharmacol.* **2004**, *55* (3), 503−517.
(32) Wang, D.; Tan, Z.; Yang, J.; Li, L.; Li, H.; Zhang, H.; Liu, H.; Liu, Y.; Wang, L.; Li, Q.; Guo, H. Perfluorooctane sulfonate promotes atherosclerosis by modulating M1 polarization of macrophages through the NF-kappaB pathway. *Ecotox. Environ. Safe.* **2023**, *249*, 114384.
(33) Qian, Y.; Ducatman, A.; Ward, R.; Leonard, S.; Bukowski, V.; Lan, G. N.; Shi, X.; Vallyathan, V.; Castranova, V. Perfluorooctane sulfonate (PFOS) induces reactive oxygen species (ROS) production in human microvascular endothelial cells: role in endothelial permeability. *J. Toxicol. Env. Health Part A* **2010**, *73* (12), 819−836.
(34) Liao, Y.; Wang, J.; Huang, Q. S.; Fang, C.; Kiyama, R.; Shen, H.; Dong, S. Evaluation of cellular response to perfluorooctane sulfonate in human umbilical vein endothelial cells. *Toxicol. Vitro.* **2012**, *26* (3), 421−428.
(35) Hu, J.; Lyu, Y.; Chen, H.; Cai, L.; Li, J.; Cao, X.; Sun, W. Integration of target, suspect, and nontarget screening with risk modeling for per- and polyfluoroalkyl substances prioritization in surface waters. *Water Res.* **2023**, *233*, 119735.
(36) Nickerson, A.; Rodowa, A. E.; Adamson, D. T.; Field, J. A.; Kulkarni, P. R.; Kornuc, J. J.; Higgins, C. P. Spatial Trends of Anionic, Zwitterionic, and Cationic PFASs at an AFFF-Impacted Site. *Environ. Sci. Technol.* **2021**, *55* (1), 313−323.
(37) Deng, P.; Durham, J.; Liu, J.; Zhang, X.; Wang, C.; Li, D.; Gwag, T.; Ma, M.; Hennig, B. Metabolomic, Lipidomic, Transcriptomic, and Metagenomic Analyses in Mice Exposed to PFOS and Fed Soluble and Insoluble Dietary Fibers. *Environ. Health Perspect.* **2022**, *130* (11), 117003.
(38) Cong, X.; Kong, W. Endothelial tight junctions and their regulatory signaling pathways in vascular homeostasis and disease. *Cell. Signal.* **2020**, *66*, 109485.
(39) Mehta, A.; Shapiro, M. D. Apolipoproteins in vascular biology and atherosclerotic disease. *Nat. Rev. Cardiol.* **2022**, *19* (3), 168−179.
(40) van der Vorst, E. High-Density Lipoproteins and Apolipoprotein A1. *Subcell Biochem.* **2020**, *94*, 399−420.
(41) Go, G. W.; Mani, A. Low-density lipoprotein receptor (LDLR) family orchestrates cholesterol homeostasis. *Yale J. Biol. Med.* **2012**, *85* (1), 19−28.
(42) Liu, B.; Zhu, L.; Wang, M.; Sun, Q. Associations between Per- and Polyfluoroalkyl Substances Exposures and Blood Lipid Levels among Adults-A Meta-Analysis. *Environ. Health Perspect.* **2023**, *131* (5), 56001.
(43) Kalyn, M.; Lee, H.; Curry, J.; Tu, W.; Ekker, M.; Mennigen, J. A. Effects of PFOS, F-53B and OBS on locomotor behaviour, the dopaminergic system and mitochondrial function in developing zebrafish (Danio rerio). *Environ. Pollut.* **2023**, *326*, 121479.
(44) Wang, Q.; Huang, J.; Liu, S.; Wang, C.; Jin, Y.; Lai, H.; Tu, W. Aberrant hepatic lipid metabolism associated with gut microbiota dysbiosis triggers hepatotoxicity of novel PFOS alternatives in adult zebrafish. *Environ. Int.* **2022**, *166*, 107351.
(45) Ye, Y.; Liu, B.; Wang, Z.; Liu, L.; Zhang, Q.; Zhang, Q.; Jiang, W. Sodium p-perfluorous nonenoxybenzene sulfonate induces ROS-mediated necroptosis by directly targeting catalase in HepG2 cells. *Sci. Total Environ.* **2024**, *910*, 168446.
(46) Zou, Y.; Wu, Y.; Wang, Q.; Wan, J.; Deng, M.; Tu, W. Comparison of toxicokinetics and toxic effects of PFOS and its novel alternative OBS in zebrafish larvae. *Chemosphere.* **2021**, *265*, 129116.
(47) Tu, W.; Martinez, R.; Navarro-Martin, L.; Kostyniuk, D. J.; Hum, C.; Huang, J.; Deng, M.; Jin, Y.; Chan, H. M.; Mennigen, J. A. Bioconcentration and Metabolic Effects of Emerging PFOS Alternatives in Developing Zebrafish. *Environ. Sci. Technol.* **2019**, *53* (22), 13427−13439.
(48) Singh, V.; Kaur, R.; Kumari, P.; Pasricha, C.; Singh, R. ICAM-1 and VCAM-1: Gatekeepers in various inflammatory and cardiovascular disorders. *Clin. Chim. Acta* **2023**, *548*, 117487.
(49) Oeckinghaus, A.; Hayden, M. S.; Ghosh, S. Crosstalk in NF-kappaB signaling pathways. *Nat. Immunol.* **2011**, *12* (8), 695−708.
(50) Liu, Y.; Zhang, Z.; Han, D.; Zhao, Y.; Yan, X.; Cui, S. Association between environmental chemicals co-exposure and peripheral blood immune-inflammatory indicators. *Front. Public Health.* **2022**, *10*, 980987.
(51) Arredondo Eve, A.; Tunc, E.; Mehta, D.; Yoo, J. Y.; Yilmaz, H. E.; Emren, S.ık V.; Akcay, F. A.ıl.ız; Madak Erdogan, Z. PFAS and their association with the increased risk of cardiovascular disease in postmenopausal women. *Toxicol. Sci.* **2024**, *200* (2), 312−323.
(52) Wang, X.; Li, B.; Zhao, W. D.; Liu, Y. J.; Shang, D. S.; Fang, W. G.; Chen, Y. H. Perfluorooctane sulfonate triggers tight junction ″opening″ in brain endothelial cells via phosphatidylinositol 3-kinase. *Biochem. Biophys. Res. Commun.* **2011**, *410* (2), 258−263.
(53) Bazzoni, G.; Dejana, E. Endothelial cell-to-cell junctions: molecular organization and role in vascular homeostasis. *Physiol. Rev.* **2004**, *84* (3), 869−901.
(54) Vestweber, D. VE-cadherin: the major endothelial adhesion molecule controlling cellular junctions and blood vessel formation. *Arterioscler. Thromb. Vasc. Biol.* **2008**, *28* (2), 223−232.
(55) Sedovy, M. W.; Leng, X.; Leaf, M. R.; Iqbal, F.; Payne, L. B.; Chappell, J. C.; Johnstone, S. R. Connexin 43 across the Vasculature: Gap Junctions and Beyond. *J. Vasc. Res.* **2023**, *60* (2), 101−113.
(56) Feldman, G. J.; Mullin, J. M.; Ryan, M. P. Occludin: structure, function and regulation. *Adv. Drug Delivery Rev.* **2005**, *57* (6), 883−917.
(57) Van Itallie, C. M.; Anderson, J. M. Claudin interactions in and out of the tight junction. *Tissue Barriers.* **2013**, *1* (3), No. e25247.
(58) McCain, J. The MAPK (ERK) Pathway: Investigational Combinations for the Treatment Of BRAF-Mutated Metastatic Melanoma. *P T.* **2013**, *38* (2), 96−108.
(59) Liu, Y.; Mu, S.; Li, X.; Liang, Y.; Wang, L.; Ma, X. Unfractionated Heparin Alleviates Sepsis-Induced Acute Lung Injury by Protecting Tight Junctions. *J. Surg. Res.* **2019**, *238*, 175−185.
(60) Fischer, S.; Wiesnet, M.; Renz, D.; Schaper, W. H2O2 induces paracellular permeability of porcine brain-derived microvascular endothelial cells by activation of the p44/42 MAP kinase pathway. *Eur. J. Cell Biol.* **2005**, *84* (7), 687−697.
(61) Chattopadhyay, R.; Dyukova, E.; Singh, N. K.; Ohba, M.; Mobley, J. A.; Rao, G. N. Vascular endothelial tight junctions and barrier function are disrupted by 15(S)-hydroxyeicosatetraenoic acid partly via protein kinase C ϵ-mediated zona occludens-1 phosphorylation at threonine 770/772. *J. Biol. Chem.* **2014**, *289* (6), 3148−3163.